Microsyst Technol (2006) 12: 208–218
DOI 10.1007/s00542-005-0057-z

TECHNICAL PAPER

Thitima Jintanawan

# Vibration of hard disk drive spindle systems with distributed journal bearing forces

Received: 8 October 2004 / Accepted: 4 May 2005 / Published online: 18 October 2005


**Abstract** This paper is to analyze vibration of fluid dynamic bearing spindles with distributed journal bearing forces. The dynamical model is developed to predict the transverse vibration of the disk–spindle systems in HDD where an aspect ratio of the bearing width to the shaft length is significant and the shaft is likely flexible. In such spindles the journal bearing functions as a continuous support, providing the *distributed* restoring and damping forces, and is therefore modeled as distributed linear spring and damping forces through distribution functions of dynamic coefficients. Vibration analysis reveals that the spindle model with distributed bearing forces predicts the same natural frequencies for all transverse modes but higher modal damping of the rocking modes, when compared to the values predicted by the conventional model with discrete bearing forces. The difference in damping prediction is clearer for the flexible-shaft spindle whose ratio of the bearing width to the shaft length becomes larger.

## 1 Introduction

Fluid dynamic bearing (FDB) spindle motors are currently used in hard disk drive (HDD) because of the FDB capability in vibration and acoustic reduction. In the FDB spindle drives, the herringbone grooved journal bearings (HGJB) are used to provide restoring and damping forces in the radial direction. In conventional approach, the dynamic forces provided by the journal bearings, including HGJBs, are modeled as discrete linear spring and damping forces acting at the bearing center (Booser 1984; Klit et al. 1986; Zirkelback et al. 1998; Jang et al. 1999).

T. Jintanawan
Department of Mechanical Engineering,
Chulalongkorn University, Bangkok, Thailand 10330
E-mail: Thitima.j@chula.ac.th

The transverse vibration of HDD spindles, occurring in the disk-plane direction, is the main cause of the track misregistration that limits the storage density performance. It has been known that the property and location of HGJB play an important role in optimizing such unwanted transverse vibration (Park et al. 2002). To develop a dynamic model predicting the vibration of the disk–spindle systems for HDD, one can observe that geometry of the bearing-spindle in HDD is quite unique; i.e., the aspect ratio of the bearing width to the shaft length is *significant* or greater when compared with that in general rotordynamic systems. Taking disk drives with small form factors (e.g., 0.85 in. HDD to be used in cell phones) as an example, most of the shaft length is supported by the bearings. In this case the aspect ratio of the width for each bearing to the shaft length could be as great as 0.5. In addition the spindle shaft in HDD is more accurately modeled as a flexible shaft than a rigid shaft (Jintanawan et al. 2001). With these observations, the HGJBs in the HDD spindles would rather function as a continuous support providing *distributed* restoring and damping forces. Jintanawan (2004) proposes a new dynamic model of distributed bearing forces in HGJB. In the paper, the distribution functions of dynamic coefficients characterizing the distributed forces of the HGJB were determined.

This paper is to further develop a dynamical model of disk–spindle systems with distributed forces in HGJB for predicting vibration in HDD. The HGJB is modeled as distributed linear spring and damping forces through distribution functions of the direct and cross-coupled spring and damping coefficients. Determination of these coefficients is presented in Sect. 2. The mathematical model of disk–spindle systems with distributed bearing forces is then developed and summarized in Sect. 3. In Sect. 4, free and forced transverse vibrations predicted by this present model are compared with those from the conventional spindle model with discrete bearing forces. How the distribution of bearing forces affects the vibration of HDD spindles is analyzed for various bearing widths.

## 2 Determination of distribution of dynamic bearing coefficients

Consider an arbitrary HGJB as shown in Fig. 1. There exists two types of HGJB for HDD spindles depending on the location of their grooves: (a) the grooved-bearing (GB) type, and (b) the grooved-journal (GJ) type. The GB type has the grooves located on the bearing sleeve, while the GJ type has the grooves located on the rotating journal. The groove angles for both types are in the opposite direction, in order to pump the fluid inward. In addition, the bearing width is $L$ and the journal having a radius $R$ rotates with a constant angular speed $\omega_3$.

To determine the dynamic coefficients of the HGJB, Reynolds equation governing a pressure field of the journal bearing is formulated. The pressure perturbation arising from the dynamic perturbations of journal displacements and velocities is then analyzed using a

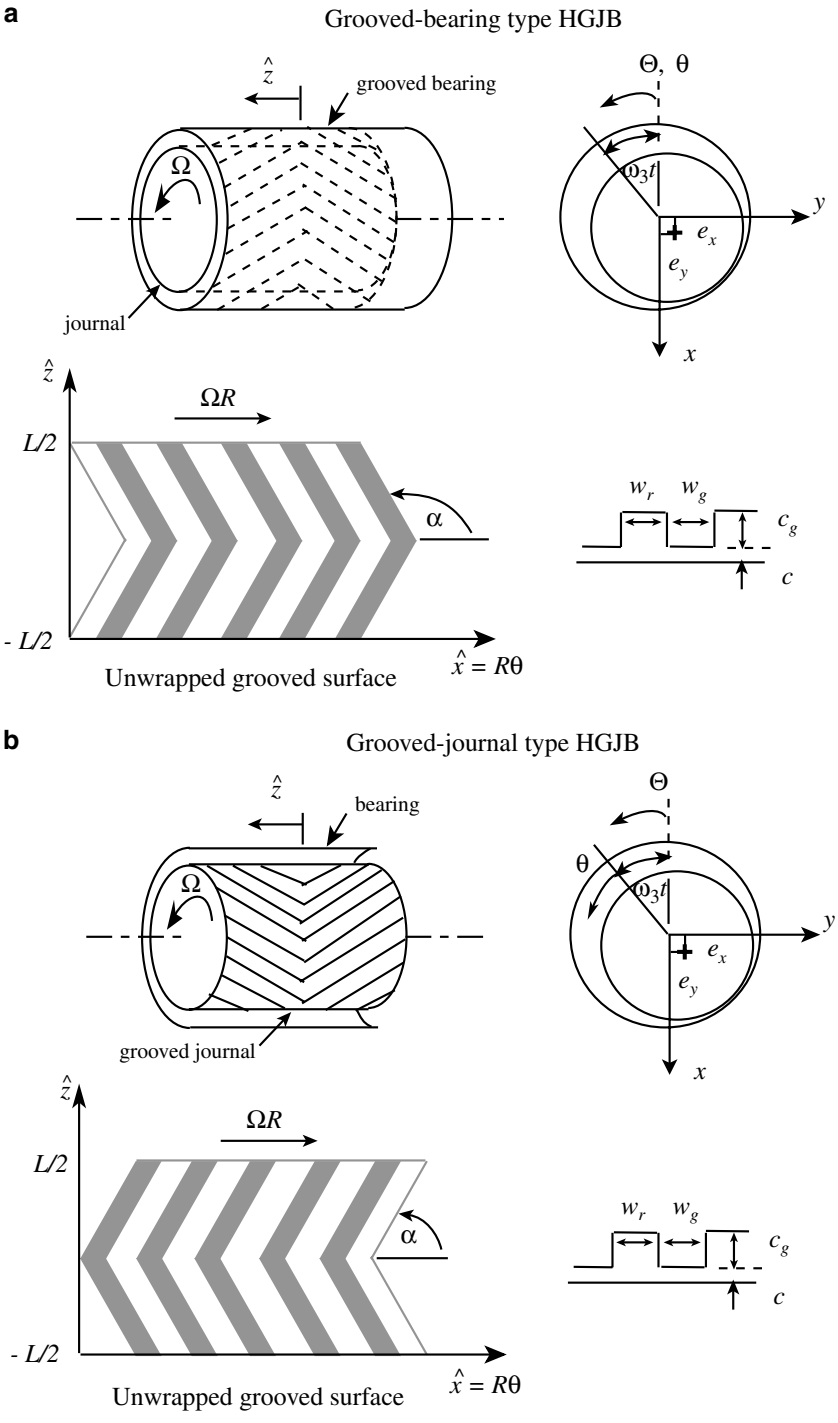


**Fig. 1** A herringbone groove journal bearing: grooved bearing type; and grooved journal type

variational approach (Klit et al. 1986). The detailed derivation of the pressure perturbation $p_x, p_y, p_{\dot{x}}$ and $p_{\dot{y}}$, with respect to the perturbation of displacements and velocities respectively, is presented in Appendix A. The finite element model is developed to subsequently solve for the steady-state pressure field and the pressure perturbation generated in the HGJB. The pressure perturbation $p_x, p_y, p_{\dot{x}}$ and $p_{\dot{y}}$ is then integrated over a circumferential direction to obtain the distribution of stiffness and damping coefficients along the bearing length. The distribution of bearing coefficients, being function of the bearing position $\hat{z}$ that measured from the bearing center along its length, are represented in a matrix form as

$$\mathbf{k} = \begin{bmatrix} k_{xx}(\hat{z}) & k_{xy}(\hat{z}) \\ k_{yx}(\hat{z}) & k_{yy}(\hat{z}) \end{bmatrix} = \int_{\theta} \begin{pmatrix} -\cos\theta \\ -\sin\theta \end{pmatrix} [p_x(\hat{z}) \quad p_y(\hat{z})] R \mathrm{d}\theta \tag{1}$$

and

$$\mathbf{c} = \begin{bmatrix} c_{xx}(\hat{z}) & c_{xy}(\hat{z}) \\ c_{yx}(\hat{z}) & c_{yy}(\hat{z}) \end{bmatrix} = \int_{\theta} \begin{pmatrix} -\cos\theta \\ -\sin\theta \end{pmatrix} [p_{\dot{x}}(\hat{z}) \quad p_{\dot{y}}(\hat{z})] R \mathrm{d}\theta, \tag{2}$$

where θ is the bearing angle, $k_{xx}(\hat{z})$ and $k_{yy}(\hat{z})$ denote the direct stiffness distributions, $k_{xy}(\hat{z})$ and $k_{yx}(\hat{z})$ denote the cross-coupled stiffness distributions, $c_{xx}(\hat{z})$ and $c_{yy}(\hat{z})$ denote the direct damping distributions, and $c_{xy}(\hat{z})$ and $c_{yx}(\hat{z})$ denote the cross-coupled damping distributions. The distributions of stiffness and damping coefficients in (1) and (2) have units of $\mathrm{N/m^2}$ and $\mathrm{Ns/m^2}$, respectively, characterizing the distributed bearing forces. Note that total stiffness and damping coefficients for the discrete bearing forces can be determined from an integration of $k_{xx}(\hat{z}), k_{xy}(\hat{z}), c_{xx}(\hat{z})$, and $c_{xy}(\hat{z})$ over $\hat{z}$.

In general, the data of the bearing coefficients for HGJB in spindle drives are determined numerically in terms of discrete stiffness and damping coefficients, and these data are reported in various publications. Thus, the present model of distributed bearing forces was validated by comparing the *total* dynamic coefficients for the discrete bearing forces of various HGJBs with the data published in Zirkelback et al. (1998) and Jang et al. (1999), as presented in Jintanawan (2004). The difference of the bearing coefficients in the comparison is less than 8%.

A GB-type HGJB for a HDD spindle with properties and geometry shown in Table 1 is analyzed. Figure 2 shows the distribution of dynamic coefficients of this HGJB at various bearing position $\hat{z}$. The calculation yields $k_{xx}(\hat{z}) = k_{yy}(\hat{z}), k_{xy}(\hat{z}) = -k_{yx}(\hat{z}), c_{xx}(\hat{z}) = c_{yy}(\hat{z})$, and $c_{xy}(\hat{z}) = -c_{yx}(\hat{z})$. This so-called isotropic property occurs in the lightly loaded bearing such as the HGJB for hard disk drives. In Fig. 2, the distributions of direct and cross-coupled stiffness $k_{xx}(\hat{z}), k_{xy}(\hat{z})$ and the distribution of direct damping $c_{xx}(\hat{z})$ are gradually increased from both sided-ends of the bearing, and reach maximum at the bearing center. In addition the cross-coupled stiffness $k_{xy}(\hat{z})$ is larger than the direct stiffness $k_{xx}(\hat{z})$. Note that the total cross-coupled damping is about zero.

**Table 1** Geometry and property of the GB-type HGJB

| | |
|---|---|
| Fluid viscosity (μ) | 0.0142 Pa's |
| Clearance ($c$) | 2.5 μm |
| Rotational speed ($\omega_3$) | 7,200 rpm |
| Radius of journal ($R$) | 2 mm |
| Groove angle ($\alpha$) | 157° |
| Groove depth ratio ($c_g/c$) | 2.4 |
| Ridge ratio ($w_r/w_r + w_g$) | 0.8 |
| Number of groove ($N_g$) | 6 |
| Bearing width to diameter ratio ($L/D$) | 0.7 |
| Eccentricity ratio ($e_0/c$) | 0 |

## 3 Dynamical model of FDB spindle systems with distributed bearing forces

In this section, the mathematical model of fluid dynamic bearing (FDB) spindle systems with distributed journal bearing forces, predicting the *transverse* vibration of a HDD, is presented. The equations governing the transverse motion of the spindle systems are derived using Lagrange's method. Most detailed derivation is not different from that presented in Jintanawan et al. (2001) and would be omitted here. This paper however will focus on a formulation of the distributed bearing forces provided by HGJB and a contribution of these distributed forces to the dynamical model of the system.

### 3.1 Model description

Figure 3 shows a physical model of the FDB spindle system in HDD. The system consists of $N$ elastic circular disks clamped to a deformable hub that allows infinitesimal rigid-body translation and rocking. The hub is press-fit onto a *rotating*, *flexible* shaft, which is mounted to the base through two HGJB and a spiral-grooved thrust bearing. The HGJBs provide *distributed* direct and cross-coupled spring and damping forces in the radial direction. The thrust bearing provides the axial restoring and damping forces against the spindle axial motion as well as the restoring- and damping-rocking moments against the spindle rocking. In order to provide the rocking moment to the system, the thrust bearing is modeled as torsional springs and dampers through the angular direct and cross-coupled stiffness and damping coefficients, $k_{t1}$, $k_{t2}$, $c_{t1}$, $c_{t2}$ (Jintanawan et al. 2001). According to large deformation of the hub around the press-fit, the hub-shaft interface is modeled as a hinged support with a torsional spring. In this model, the spindle system is axisymmetric and all the disks are identical. Only the zero-nodal-circle modes of the disk vibration are retained in the

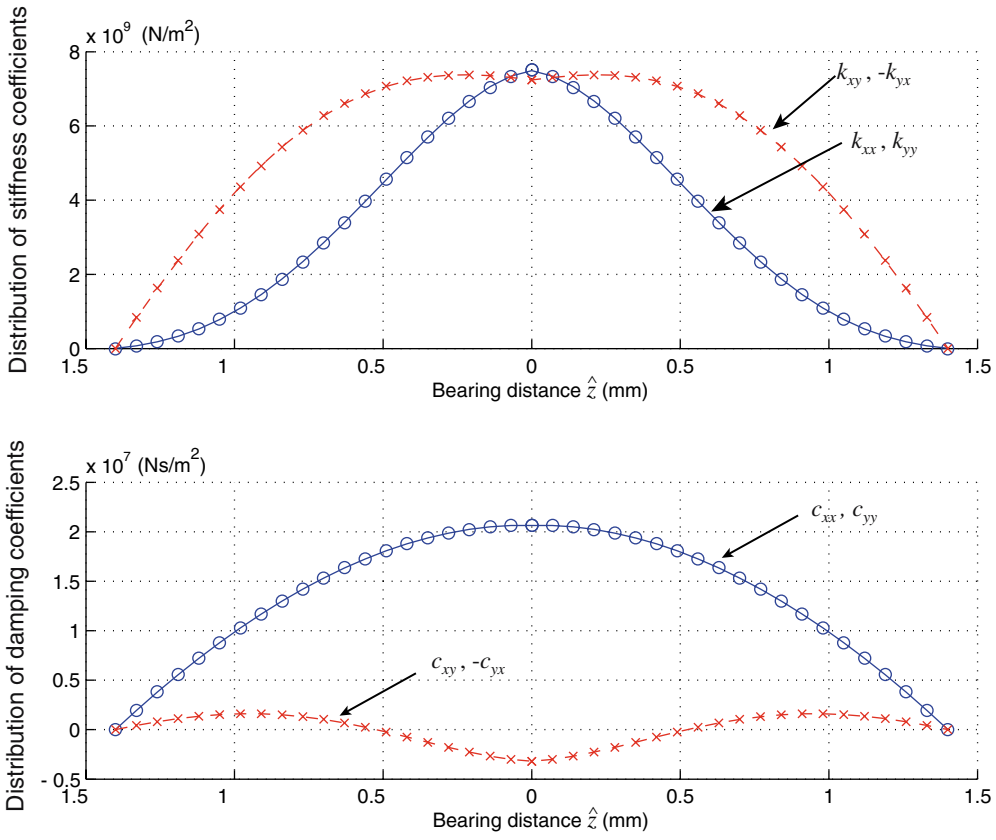


**Fig. 2** Distributions of dynamic coefficients of the GB-type HGJB

mathematical model because of their significance in the frequency range of interest. Moreover, the motion of the system in the spindle's transverse and axial directions can be completely decoupled (Jintanawan 2000). In this study, the spindle spins at a constant speed $\omega_3$ and is subjected to the base excitation in the disk-plane direction, thus the system exhibits only the transverse motion.

The transverse motion of the FDB spindle system for HDD is described by the following generalized coordinates: infinitesimal rigid body whirling of the spindle hub ($R_x$, $R_y$); infinitesimal rigid body precession of the hub ($\theta_x$, $\theta_y$); eigenmodes of the flexible shaft ($q_x$, $q_y$); and the (0,1) eigenmodes of each disk $(q_{01}^{(i)}, q_{0,-1}^{(i)}, i = 1, 2, ..., N)$.

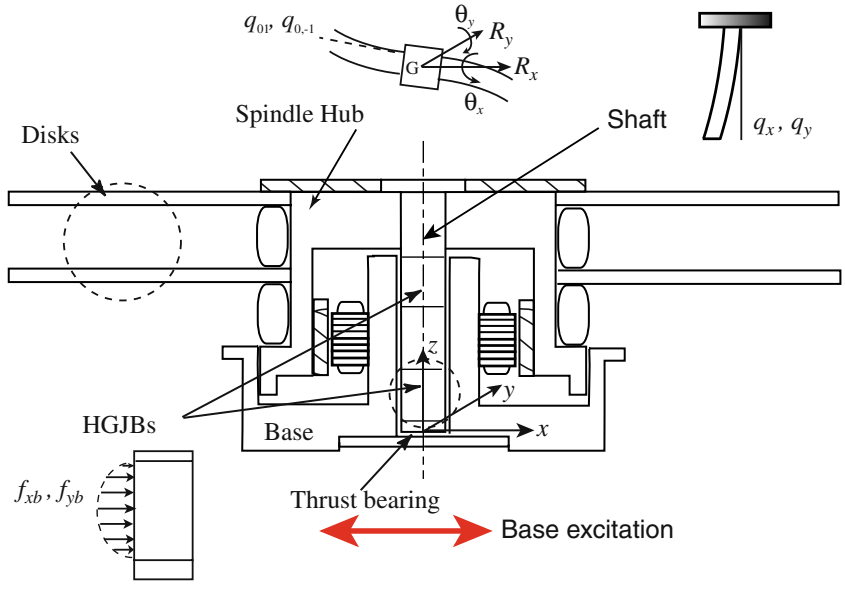


**Fig. 3** A FDB spindle system for HDD

### 3.2 Model of distributed dynamic bearing forces in HGJB

The HGJB is modeled as generalized internal forces through distributed direct and cross-coupled stiffnesses and dampings. Let us consider a single arbitrary HGJB. An infinitesimal deflection of the bearing at various position $z$, ($z$ is measured from the lower end of the shaft), can be discretized in terms of the generalized coordinates as follows:

$$\begin{aligned}\mathbf{r}_b(z) &\equiv r_{xb}(z)\mathbf{I} + r_{yb}(z)\mathbf{J} + r_{zb}\mathbf{K}; \quad z_{\mathrm{lb}} \leqslant z \leqslant z_{\mathrm{ub}} \\ &= (R_x + \phi(z)q_x + z_b\theta_y)\mathbf{I} + (R_y + \phi(z)q_y - z_b\theta_x)\mathbf{J} \\ &\quad + R_z\mathbf{K}, \end{aligned} \tag{3}$$

where **I, J** and **K** are the unit vectors, $\phi$ ($z$) is the first modeshape or eigenfunction of the shaft, $z_{\mathrm{lb}}$ and $z_{\mathrm{ub}}$ are the positions of lower and upper ends of the bearing, and $z_b = z - z_G$ is the bearing position that measured with respect to the system C.G. For the isotropic bearing, the distribution of stiffness and damping coefficients are simply

$$\begin{aligned} k_1(z) &\equiv k_{xx}(z) = k_{yy}(z); \quad k_2(z) \equiv k_{xy}(z) = -k_{yx}(z); \\ c_1(z) &\equiv c_{xx}(z) = c_{yy}(z); \quad c_2(z) \equiv c_{xy}(z) = -c_{yx}(z) \end{aligned}. \tag{4}$$

With $k_1(z)$, $k_2(z)$, $c_1(z)$, and $c_2(z)$ obtained from Section 2, the distributed forces per unit length provided by HGJB are

$$\begin{aligned}\begin{pmatrix} f_{xb}(z) \\ f_{yb}(z) \end{pmatrix} &= -\begin{bmatrix} k_1(z) & k_2(z) \\ -k_2(z) & k_1(z) \end{bmatrix}\begin{pmatrix} r_{xb}(z) \\ r_{yb}(z) \end{pmatrix} \\ &\quad - \begin{bmatrix} c_1(z) & c_2(z) \\ -c_2(z) & c_1(z) \end{bmatrix}\begin{pmatrix} \dot{r}_{xb}(z) \\ \dot{r}_{yb}(z) \end{pmatrix}. \end{aligned} \tag{5}$$

Hence the virtual work done by HGJB is

$$\delta W = \int_{z_{\mathrm{lb}}}^{z_{\mathrm{ub}}} f_{xb}(z)\delta r_{xb}\mathrm{d}z + \int_{z_{\mathrm{lb}}}^{z_{\mathrm{ub}}} f_{yb}(z)\delta r_{yb}\mathrm{d}z, \tag{6}$$

where $\delta r_{xb}$ ($z$) and $\delta r_{yb}$ ($z$) are virtual displacements of the bearing.

### 3.3 Equations governing transverse motion

The equation governing the transverse motion of the FDB spindle system can be simplified by using the following complex representation

$$\begin{aligned} &\bar{\theta} \equiv \theta_x + j\theta_y,\ \bar{R} \equiv R_x + jR_y, \\ &\bar{Q}_{01}^{(i)} \equiv q_{0,-1}^{(i)} - jq_{01}^{(i)},\ \bar{q} \equiv q_x + jq_y \end{aligned}, \tag{7}$$

where $j \equiv \sqrt{-1}$. The matrix equation of motion governing the transverse motion of the system is then

$$M\ddot{\mathbf{q}}(t) + (\mathbf{G} + \mathbf{C})\dot{\mathbf{q}}(t) + \mathbf{K}\mathbf{q}(t) = \mathbf{f}(t), \tag{8}$$

where **q** is a vector of the generalized coordinates, **M** is the inertia matrix, **G** is the complex gyroscopic matrix, **C** is the complex damping matrix, and **K** is the complex stiffness and oscillatory matrix given by

$$\mathbf{q} = \left(\bar{\theta},\ \bar{R},\ \bar{q},\ \bar{Q}_{01}^{(1)},\ \bar{Q}_{01}^{(2)},\ \ldots,\ \bar{Q}_{01}^{(N)}\right)^{\mathrm{T}}, \tag{9}$$

$$\mathbf{M} = \begin{bmatrix} \eta_1 & 0 & j\alpha_1 & a_0 & a_0 & \cdots & a_0 \\ 0 & \eta_0 & \lambda_1 & 0 & 0 & \cdots & 0 \\ -j\alpha_1 & \lambda_1 & \eta_2 & 0 & 0 & \cdots & 0 \\ a_0 & 0 & 0 & 1 & 0 & \cdots & 0 \\ a_0 & 0 & 0 & 0 & 1 & \cdots & 0 \\ \vdots & \vdots & \vdots & \vdots & \vdots & \ddots & \vdots \\ a_0 & 0 & 0 & 0 & 0 & \cdots & 1 \end{bmatrix}, \tag{10}$$

$$\mathbf{G} = j\omega_3\begin{bmatrix} \eta_3 & 0 & j\alpha_2 & 2a_0 & 2a_0 & \cdots & 2a_0 \\ 0 & 0 & 0 & 0 & 0 & \cdots & 0 \\ -j\alpha_2 & 0 & \lambda_2 & 0 & 0 & \cdots & 0 \\ 2a_0 & 0 & 0 & 2 & 0 & \cdots & 0 \\ 2a_0 & 0 & 0 & 0 & 2 & \cdots & 0 \\ \vdots & \vdots & \vdots & \vdots & \vdots & \ddots & \vdots \\ 2a_0 & 0 & 0 & 0 & 0 & \cdots & 2 \end{bmatrix}, \tag{11}$$

$$\mathbf{C} = \begin{bmatrix} c_{\theta\theta} & c_{\theta R} & c_{\theta q} & 0 & 0 & \cdots & 0 \\ -c_{\theta R} & c_{RR} & c_{Rq} & 0 & 0 & \cdots & 0 \\ -c_{\theta q} & c_{Rq} & c_{qq} & 0 & 0 & \cdots & 0 \\ 0 & 0 & 0 & 0 & 0 & \cdots & 0 \\ 0 & 0 & 0 & 0 & 0 & \cdots & 0 \\ \vdots & \vdots & \vdots & \vdots & \vdots & \ddots & \vdots \\ 0 & 0 & 0 & 0 & 0 & \cdots & 0 \end{bmatrix}, \tag{12}$$

$$\mathbf{K} = \begin{bmatrix} k_{\theta\theta} & k_{\theta R} & k_{\theta q} & 0 & 0 & \cdots & 0 \\ -k_{\theta R} & k_{RR} & k_{Rq} & 0 & 0 & \cdots & 0 \\ -k_{\theta q} & k_{Rq} & k_{qq} & 0 & 0 & \cdots & 0 \\ 0 & 0 & 0 & k_{01} & 0 & \cdots & 0 \\ 0 & 0 & 0 & 0 & k_{01} & \cdots & 0 \\ \vdots & \vdots & \vdots & \vdots & \vdots & \ddots & \vdots \\ 0 & 0 & 0 & 0 & 0 & \cdots & k_{01} \end{bmatrix}, \tag{13}$$

**f**($t$) is a vector of the generalized forces associated with the base acceleration $\ddot{s}(t)$ given by

$$\mathbf{f} = \ddot{s}(t)(0,\ \eta_0,\ \lambda_1,\ 0,\ \ldots,\ 0)^{\mathrm{T}}. \tag{14}$$

The distributions of coefficients $k_1(z)$, $k_2(z)$, $c_1(z)$, and $c_2(z)$ are contributed to the components of matrices **C** and **K** in (12) and (13) as follows:

$$\begin{aligned} c_{\theta\theta} &= \frac{1}{I_1}\sum_r \left[\int_{z_{\mathrm{lb}}}^{z_{\mathrm{ub}}} z_b^2(c_1 - jc_2)\mathrm{d}z\right] + \sum_t C_t, \\ c_{\theta R} &= \frac{j}{I_1}\sum_r \left[\int_{z_{\mathrm{lb}}}^{z_{\mathrm{ub}}} z_b(c_1 - jc_2)\mathrm{d}z\right] \end{aligned} \tag{15}$$

$$c_{\theta q} = \frac{j}{I_1}\sum_r \left[\int_{z_{lb}}^{z_{ub}} z_b\phi(z)(c_1 - jc_2)\mathrm{d}z\right] + \sum_t \frac{\partial\phi(z_t)}{\partial z} C_t,$$

$$c_{RR} = \frac{1}{I_1}\sum_r \left[\int_{z_{lb}}^{z_{ub}} (c_1 - jc_2)\mathrm{d}z\right],$$

$$c_{Rq} = \frac{1}{I_1}\sum_r \left[\int_{z_{lb}}^{z_{ub}} \phi(z)(c_1 - jc_2)\mathrm{d}z\right],$$

$$c_{qq} = \frac{1}{I_1}\sum_r \left[\int_{z_{lb}}^{z_{ub}} \phi^2(z)(c_1 - jc_2)\mathrm{d}z\right] + \sum_t \left[\frac{\partial\phi(z_t)}{\partial z}\right]^2 C_t$$

where $\sum_r []$ and $\sum_t []$ are sum over all the radial HGJBs and the thrust bearings, respectively, $C_t = c_{t1} - jc_{t2}$ is the angular damping coefficients of the thrust bearing, and $z_t$ is the position of the thrust bearing. In addition, the coefficients $k_{\theta\theta}$, $k_{\theta R}$, $k_{\theta q}$, $k_{RR}$, $k_{Rq}$ can be found from (15) with all $c$ replaced by $k$. Also

$$k_{qq} = \omega_s^2 + \frac{1}{I_1}\sum_r \left[\int_{z_{lb}}^{z_{ub}} \phi^2(z)(k_1 - jk_2)\mathrm{d}z\right] + \sum_t \left[\frac{\partial\phi(z_t)}{\partial z}\right]^2 K_t, \quad (16)$$

where $\omega_s$ is the shaft natural frequency, and $K_t = k_t - jk_{t2}$ is the angular stiffness coefficients of the thrust bearing. Moreover, the rest detailed description of each term in **M**, **G**, **C**, **K**, and **f**($t$) is given in Appendix B.

## 4 Vibration analysis

In this section, free and forced vibrations of the FDB spindle systems with distributed bearing forces are analyzed for various aspect ratios of the bearing width to the shaft length. For the free vibration, natural frequencies and modal dampings of the transverse modes are present. The modal damping indicates the shape of resonance peak and characteristics of the resonance amplitudes when subjected to the excitation. For forced vibration, transverse frequency response functions (FRF) of the system subjected to the base excitation in the disk-plane direction are present. Free and forced vibrations predicted by the model in Sect. 3 are compared to those predicted by the conventional model with discrete bearing forces (Jintanawan et al. 2001). Effect of the distributed bearing forces of HGJBs on the natural frequencies, modal dampings and transverse FRF of the spindle system is then discussed.

Two nearly identical disk–spindle systems $A$ and $B$ for HDD, with only difference in bearing width, are studied. Both systems have two-disk platter. Geometries and properties of the disks and spindle are listed in Table 2. Each spindle consists of two identical HGJB whose property and geometry, except $L/D$, are previously shown in Table 1. In addition the bearing width of spindles $A$ and $B$ are 2.8 and 5 mm, respectively. Thus the aspect ratios of each bearing width to the shaft length for both spindles are 0.17 and 0.30, respectively. The angular stiffness and damping coefficients of the thrust bearing are assumed small and negligible in this case.

### 4.1 Free vibration

The model of spindle system with distributed bearing forces developed in Sect. 3 predicts the natural frequencies and the modal dampings of spindles $A$ and $B$ as illustrated by the solid lines in Fig. 4 for various spin speeds. In addition, these results are compared to the values predicted by the model with discrete bearing forces as shown by the dashed lines in the same plot. Furthermore, the values of the natural frequencies and the modal dampings of spindles $A$ and $B$ for 120 Hz spin speed that predicted by both models are presented in Tables 3 and 4. Both spindle models with either discrete or distributed bearing forces predict *similar* characteristics of the transverse vibration which can be divided into two groups: (a) four half-speed whirl (HSW) modes, and (b) two pairs of rocking modes; see Fig. 4. Each modeshape exhibits a coupled motion of the spindle whirling and precession, the flexible shaft vibration and

**Table 2** Geometry and properties of a two-disk FDB spindle system in a hard disk drive

| Disk | | Spindle | |
|---|---|---|---|
| $b$ | 47.50 mm | $I_1$ | 3.293 kg mm$^2$ |
| $a$ | 15.24 mm | $I_3$ | 4.818 kg mm$^2$ |
| $I_1$ | 1.372 kg mm$^2$ | $m$ | $3.180\times10^{-2}$ kg |
| $z_1$ | −4.425 mm | Shaft | |
| $z_2$ | −8.245 mm | Length $l_s$ | 16.9 mm |
| $m$ | $2.282\times10^{-2}$ kg | Diameter $d_s$ | 4 mm |
| | | $z_{lb}$ (for lower HGJB) | 1.55 mm |
| | | $z_{ub}$ (for upper HGJB) | 14.87 mm |
| | | $E_s$ | 190 GPa |
| | | $\rho_s$ | 7,800 kg/m$^3$ |

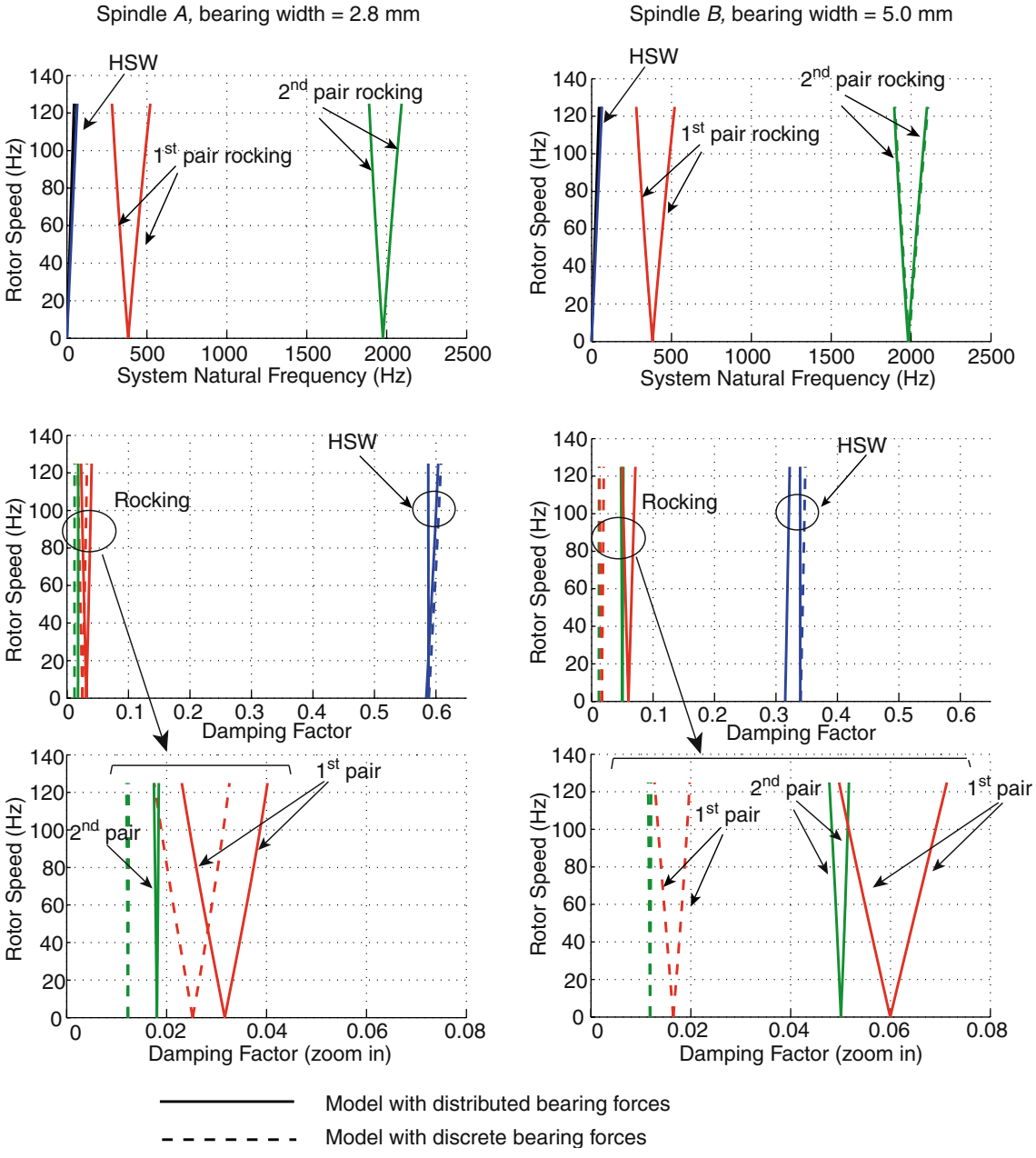


**Fig. 4** Natural frequency and modal damping of the disk–spindle system predicted by two different models: with distributed bearing forces and with discrete bearing forces, for the bearing width of 2.8 and 5.0 mm

the disk vibration of (0,1) modes (Shen et al. 1997; Jintanawan et al. 1999). All these vibration modes exist in the transverse direction, and hence are the main cause of the track misregistration. In Fig. 4, the half-speed whirls occur at a certain frequency about half of the rotor speed, and they are heavily damped compared to the rocking modes. The frequencies and damping of the rocking mode pairs have two split branches known as backward (B) and forward (F) modes, as seen in Fig. 4. In addition, for both rocking mode pairs, the modal damping of the backward modes is always slightly greater than the damping of the forward modes as shown in Tables 3 and 4. In practice, the predictable half-speed whirl can be corrected by the servo system in HDD. Therefore, it is the rocking modes that are the major concern in optimizing the vibration performance of HDD spindles. Moreover, only the spindle model considering the shaft and disk flexibility can predict these two rocking mode pairs.

Compared to the conventional model of discrete bearing forces, the spindle model with distributed bearing forces predicts the same natural frequencies for all transverse modes but predicts higher modal dampings of the rocking mode pairs. The difference in damping

**Table 3** Natural frequencies and modal dampings of spindle *A* (bearing width = 2.8 mm)

| Vibration modes | Natural frequencies (Hz) | | Modal damping (%) | |
|---|---|---|---|---|
| | Discrete model | Distributed model | Discrete model | Distributed model |
| HSW | 62.5 | 62.5 | 60 | 60 |
| Rocking B1 | 285 | 285 | 3.23 | 3.99 |
| Rocking F1 | 515 | 515 | 1.78 | 2.33 |
| Rocking B2 | 1893 | 1893 | 1.24 | 1.84 |
| Rocking F2 | 2089 | 2088 | 1.20 | 1.75 |

**Table 4** Natural frequencies and modal dampings of spindle *B* (bearing width = 5.0 mm)

| Vibration modes | Natural frequencies (Hz) | | Modal damping (%) | |
|---|---|---|---|---|
| | Discrete model | Distributed model | Discrete model | Distributed model |
| HSW | 62 | 62 | 34 | 32 |
| Rocking B1 | 282 | 283 | 1.97 | 7.09 |
| Rocking F1 | 513 | 514 | 1.29 | 5.01 |
| Rocking B2 | 1902 | 1897 | 1.20 | 5.16 |
| Rocking F2 | 2100 | 2094 | 1.15 | 4.78 |

prediction is clearer for spindle *B* where the ratio of the bearing width to the shaft length becomes larger. It implies that under the base excitation, the resonance peaks of the rocking modes predicted by the model with distributed bearing forces are more heavily damped (the peaks are less steep) and the rocking amplitude is smaller when compared to those predicted by the conventional model of discrete bearing force. In the spindle design, the rocking amplitudes have to be minimized in order to optimize the vibration performance. With the higher modal damping of the rocking modes, the vibration performance of HDD spindles is better.

The same predictions of natural frequency for both models can be explained as follows. The half-speed whirls are an inherence whirl phenomena of the bearing and their resonance frequency is only affected by the spin speed. Furthermore, the frequencies of the rocking mode pairs substantially depend on the natural frequencies of the shaft and disk ($\omega_s$ and $\omega_{01}$) through the terms $k_{qq}$ and $k_{01}$ in (13) and (16). Accordingly, the bearing property and geometry has no great effect on all resonance frequencies. The difference in damping predictions of the rocking modes from the two models can be discussed as follows. The modal damping of the rocking modes is mainly affected by the damping in the bearing as well as the bearing deflection, through the terms $c_{\theta\theta}$, $c_{\theta R}$, $c_{\theta q}$, $c_{RR}$, $c_{Rq}$, and $c_{qq}$ in (15). For the distributed bearing forces, the bearing deflection is considered as continuously varied along the bearing length due to the shaft flexibility. Thus, it results in different values of modal dampings compared to those predicted by the spindle model with discrete bearing forces that the bearing deflection is simply evaluated at the bearing center.

To further investigate the effect of shaft flexibility on the modal damping that predicted by the model with distributed bearing forces, Fig. 5 compares the natural frequencies and modal dampings[1] of two different flexible-disk spindle systems: (1) with rigid shaft; and (2) with flexible shaft, for various spin speed. When compared to the flexible-shaft system, the system with rigid shaft possesses four half-speed whirl modes but only one pair of rocking modes. This is because of reduced degrees of freedom in the system. Moreover, the modal dampings of rocking modes for the rigid-shaft spindle system, predicted by the models with either discrete or distributed bearing forces, are nearly identical, as seen on the left of Fig. 5. It is implied that the model of distributed bearing forces does not cause any difference in damping prediction unless the shaft is flexible. For the rigid shaft, the deflection of the bearing, which is affected by only the whirling and the rocking of the rigid spindle, slightly varies along its length. In such case, the dynamic resultants of bearing forces obtained from either discrete or distributed models are not different, and hence resulting in similar vibration characteristics.

For the FDB spindle system with significant aspect ratio of the bearing width to the shaft length and the shaft is likely flexible, the conventional spindle model with discrete bearing forces would not accurately predict the modal damping of rocking modes. In such system, the dynamic model of disk–spindle system with distributed bearing forces could be the alternative model for improving the damping prediction.

## 4.2 Forced vibration

In this section, we present a simulation of frequency response functions (FRF) whose response is measured from the disk along the radial or transverse direction,

[1] For all cases, the modal dampings of the half-speed whirl modes are not different, and hence they are not shown in Fig. 5

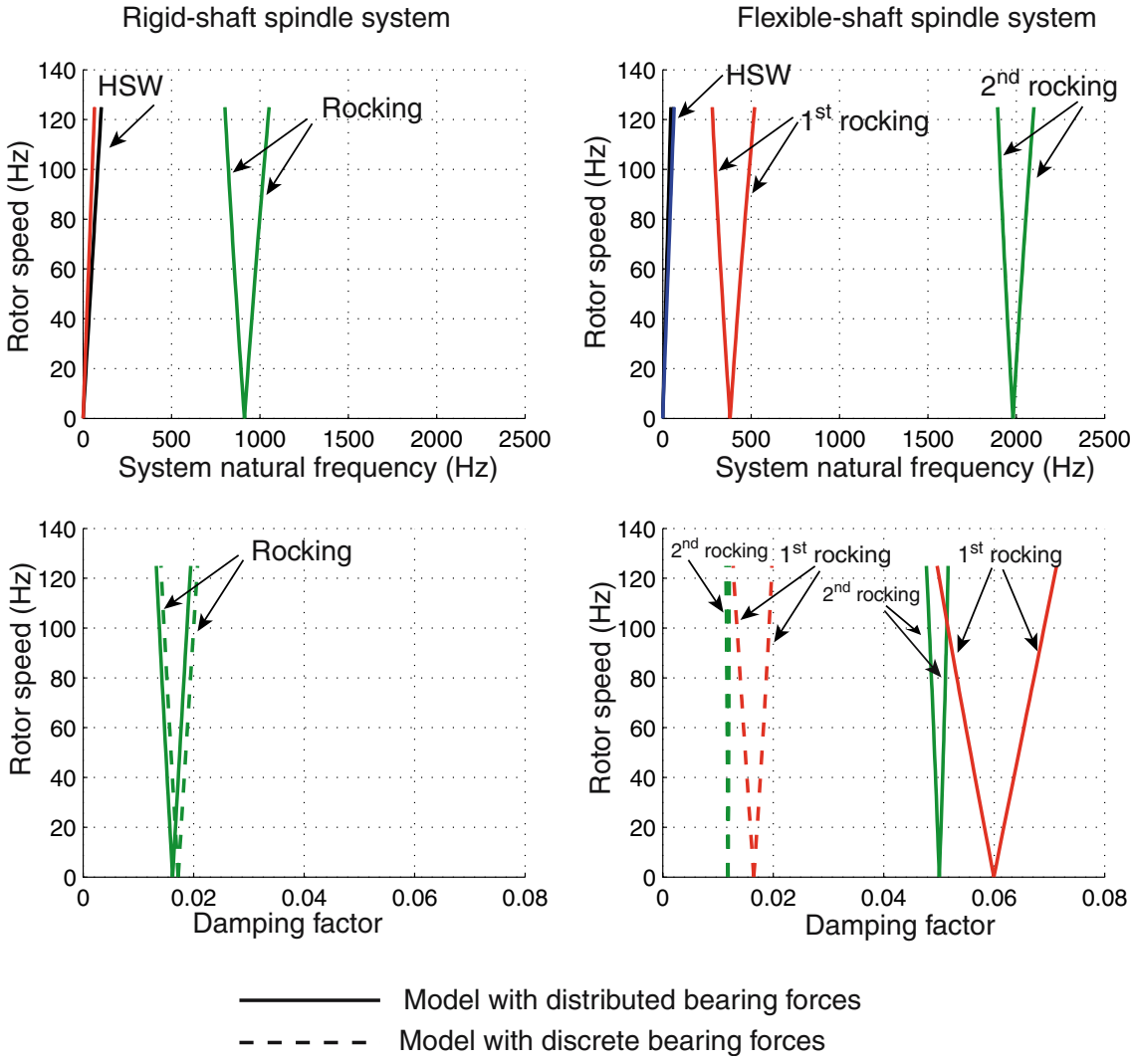


**Fig. 5** Free vibration prediction of the rigid-shaft and flexible-shaft spindle systems with the bearing width of 5.0 mm

when subjected to the base excitation in the disk-plane direction. This transverse FRF well represents the possible track-misregistration in HDD and can be expressed as:

$$\begin{aligned}\vec{\Delta}(z) &\equiv \Delta_x(z)\mathbf{I} + \Delta_y(z)\mathbf{J} \\ &= (R_x + z_0\theta_y)\mathbf{I} + (R_y - z_0\theta_x)\mathbf{J}\end{aligned}, \tag{17}$$

where $z_0 = z - z_G$ is the distance of the measurement level from system C.G. This transverse vibration consists of two components: one from the spindle whirling ($R_x$ and $R_y$) and the other from the spindle precession ($z_0\theta_y$ and $z_0\theta_x$).

Figure 6 shows the magnitudes of transverse FRF $\left|\vec{\Delta}\right|$ of the previously described disk–spindle systems *A* and *B*, when the response is measured from the lower disk and the spindle spins at 7,200 rpm or 120 Hz. In Fig. 6 the transverse FRF of both systems *A* and *B* that predicted by the spindle models with discrete and distributed bearing forces are compared. In all cases, for the frequency range of 0–800 Hz there exist the resonance peaks of half-speed whirl modes at 60 Hz and the first pair of backward and forward rocking modes at 270 and 520 Hz. Moreover, the resonance peaks of rocking modes predicted by the present model with distributed bearing forces are more heavily damped. The larger damping of rocking modes is much clearer for the case of system *B* with wider bearing width.

Note that the resonance peak of the half-speed whirls at 60 Hz as presented in Fig. 6 is more heavily damped when qualitatively compared to the peaks from general test results (e.g., Fig. 8 in Jintanawan et al. 2001). The observation reveals that the predicted modal damping of the half-speed whirl might be too high. In the parametric study (Park et al. 2002), the half-speed whirl damping is decreased with the lower direct stiffness of HGJB. Similarly, the damping of the half-speed whirl might decrease due to the flexibility of the stationary base (Tseng et al. 2003), which is not included in this model. The base flexibility would yield less stiffness of the structure

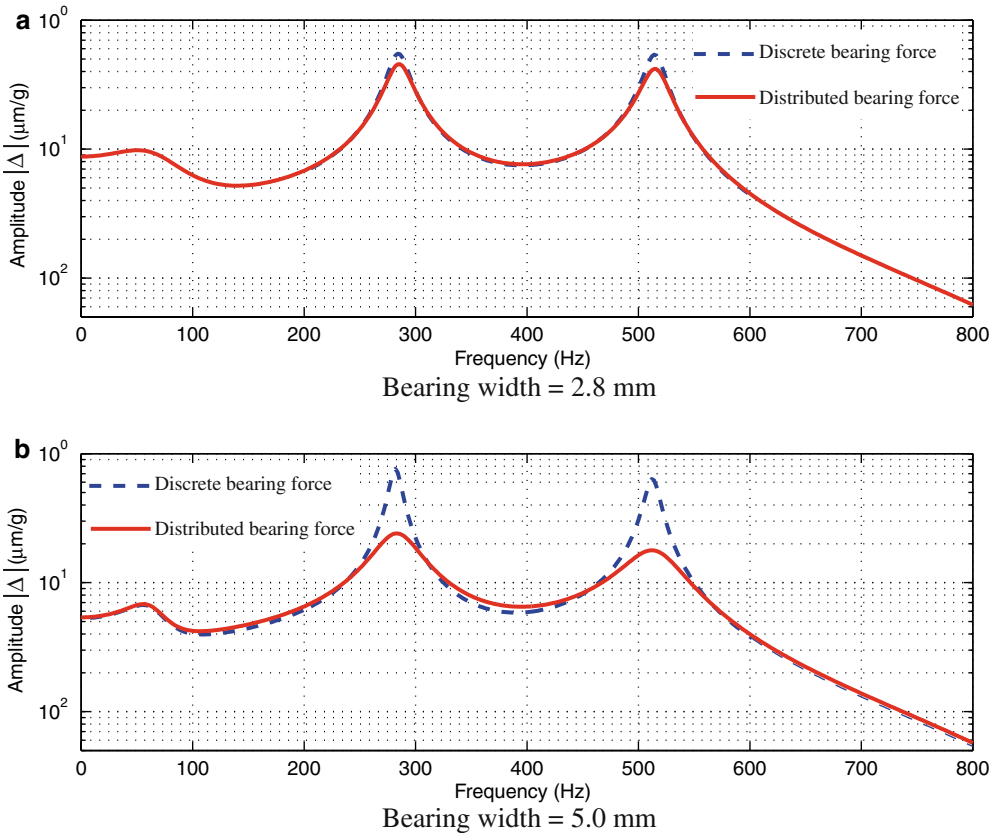


**Fig. 6** Transverse FRF of the disk–spindle system predicted by two different models: with distributed bearing forces and with discrete bearing forces, for the bearing width of 2.8 and 5.0 mm

that leads to the smaller damping of the half-speed whirl mode for the actual system. In addition, to accurately predict the half-speed whirls, the exact values of bearing properties such as viscosity, clearance, and length, etc., are needed for calculating the bearing coefficients.

## 5 Conclusions

In this paper we present a dynamical model of disk–spindle systems with *distributed* forces in HGJB for predicting transverse vibration of HDD spindles. When compared to vibration predicted by the conventional spindle model with discrete bearing forces, the present model with distributed bearing forces predicts the same natural frequencies for all transverse modes but higher modal damping of the rocking modes. The difference in damping prediction is clearer when the aspect ratio of the bearing width to the shaft length becomes larger and the shaft is likely flexible. Specifically, the modal damping of the rocking modes is substantially affected by the journal bearing forces. For the present model, these bearing forces are distributed along the bearing length where the bearing deflection is continuously varied due to the shaft flexibility. The spindle model with distributed bearing forces could be the alternative model for improving the damping prediction of the rocking modes.

**Acknowledgments** The valuable discussion from Prof. I. Y. (Steve) Shen, Department of Mechanical Engineering, University of Washington, is gratefully acknowledged. This research is supported by the "Research Grant for New Scholars-MRG4880174" from Thailand Research Fund (TRF).

## Appendix A

Consider an arbitrary herringbone grooved journal bearing (HGJB) as shown in Fig. 1. The inertial coordinate system $xy$ describes the motion of the journal center and the coordinate system $\hat{x}\hat{z}$ where $\hat{x} = R\theta$ describes the position of the unwrapped fluid film. With the grooves moving, the $\hat{x}$-axis for the GJ-type bearing is fixed to the rotating journal. In addition it is easier to consider the journal of the GJ-type bearing as relatively stationary while the bearing sleeve rotates in the opposite direction (Zirkelback et al. 1998). The Reynolds equation governing the pressure field $p$ in HGJB is

$$\begin{aligned}\frac{1}{R^2}\frac{\partial}{\partial\theta}\left(\frac{h^3}{12\mu}\frac{\partial p}{\partial\theta}\right)+\frac{\partial}{\partial\hat{z}}\left(\frac{h^3}{12\mu}\frac{\partial p}{\partial\hat{z}}\right)&\\ = L(p) = \frac{\omega_3}{2}\frac{dh}{d\theta}+\frac{\partial h}{\partial t}, &\quad \text{for GB type}\\ = -\frac{\omega_3}{2}\frac{dh}{d\theta}+\frac{\partial h}{\partial t}, &\quad \text{for GJ type}\end{aligned} \tag{18}$$

where μ is the fluid viscosity, and $h$ is the film thickness in the ridge and groove regions expressed respectively as

$$h = c + e_x \cos\Theta + e_y \sin\Theta \tag{19}$$

and

$$h = c + c_g + e_x \cos\Theta + e_y \sin\Theta. \tag{20}$$

In (19) and (20), $c$ is the nominal film clearance, $c_g$ is groove depth, $e_x$ and $e_y$ are journal eccentricities, also $\Theta = \theta$ for the GB-type HGJB, and $\Theta = \theta + \omega_3 t$ for the GJ-type HGJB. The pressure field $p$ satisfies the following boundary conditions: $p(\theta, \hat{z}, t) = p(\theta + 2\pi, \hat{z}, t)$ and $p(\theta, L/2, \hat{z}) = p(\theta, -L/2, \hat{z}) = p_a$, where $p_a$ is the atmospheric pressure.

For a small perturbation $\Delta e_\sigma$ $(t)$, $(\sigma = x, y)$, of journal displacements from the steady state configuration $(e_{x0}, e_{y0})$, the film thickness is then

$$h = h_0 + \Delta e_x \cos\Theta + \Delta e_y \sin\Theta = h_0 + \sum_\sigma \Delta e_\sigma h_\sigma;$$
$$\sigma = x, y, \tag{22}$$

where $h_0$ is the film thickness for the steady state configuration $(e_{x0}, e_{y0})$, $h_x = \cos\Theta$, and $h_y = \sin\Theta$. With the small perturbed displacement $\Delta e_\sigma(t)$ and perturbed velocity $\Delta\dot{e}_\sigma(t), (\sigma = x, y)$, the perturbed pressure field is then

$$p = p_0 + \sum_\sigma p_\sigma \Delta e_\sigma + \sum_{\dot\sigma} p_{\dot\sigma} \Delta\dot{e}_\sigma; \quad \sigma = x, y, \tag{23}$$

where $p_\sigma$ and $p_{\dot\sigma}(\sigma = x, y)$ are pressure perturbation with respect to the perturbed displacement and velocity, respectively. Substituting (22) and (23) into (18) and neglecting the higher order terms, the differential equation governing the steady-state pressure field is obtained as

$$\begin{aligned} L(p_0) &= \tfrac{\omega_3}{2}\tfrac{dh_0}{d\theta}, \quad \text{for GB type,} \\ &= -\tfrac{\omega_3}{2}\tfrac{dh_0}{d\theta} - \Omega\left[e_{x0}\sin\Theta - e_{y0}\cos\Theta\right], \quad \text{for GJ type} \end{aligned} \tag{24}$$

Moreover for both GB- and GJ-types, the equations governing the pressure perturbation are then

$$L(p_\sigma) = \frac{\omega_3}{2}\frac{dh_\sigma}{d\theta} - \frac{1}{R^2}\frac{\partial}{\partial\theta}\left(\frac{3h_0^2 h_\sigma}{12\mu}\frac{\partial p_0}{\partial\theta}\right) - \frac{\partial}{\partial\hat{z}}\left(\frac{3h_0^2 h_\sigma}{12\mu}\frac{\partial p_0}{\partial\hat{z}}\right);$$
$$\sigma = x, y, \tag{25}$$

$$L(p_{\dot\sigma}) = h_\sigma; \quad \sigma = x, y.$$

## Appendix B

In (10) to (14), $\eta_0$, $\eta_1$, $\eta_2$, $\eta_3$, $\lambda_1$, $\lambda_2$, $\alpha_1$, $\alpha_2$, and $a_0$ are the inertias normalized with respect to the diametral mass moment of inertia of each disk $I_1$, given by

$$\begin{gathered} \eta_0 = \tfrac{M}{I_1}, \quad \eta_1 = \tfrac{\bar{I}_1}{I_1}, \quad \eta_2 = \tfrac{\hat{I}_s}{I_1}, \quad \eta_3 = \tfrac{\bar{I}_3}{I_1} \\ \lambda_1 = \tfrac{M_{s1}}{I_1}, \quad \lambda_2 = \tfrac{M_{s2}}{I_1}, \quad \alpha_1 = \tfrac{N_{s1}}{I_1}, \quad \alpha_2 = \tfrac{N_{s2}}{I_1}, \\ a_0 = \tfrac{\pi\rho h}{I_1}\int_a^b R_{01}(r) r^2 \mathrm{d}r \end{gathered} \tag{26}$$

where $M$ is the total mass of the spindle system, $\bar{I}$ and $\bar{I}_3$ are the centroidal mass moment of inertia of the rotating part about $x$ and $y$ axes, and $M_{s1}$, $M_{s2}$, $N_{s1}$, $N_{s2}$, and $\hat{I}_s$ are the modal mass of the shaft defined in Jintanawan (2000).

In (13) $k_{01} = \omega_{01}^2 - \omega_3^2 - j\zeta\omega_3$, where $\omega_{01}$ and $\zeta$ is the natural frequencies and the normalized viscous damping of the disks as defined in Jintanawan (2000).

## References


Booser ER (1984) Handbook of lubrication, volume I and II, CRC Press, Florida

Jang G, Kim Y (1999) Calculation of dynamic coefficients in hydrodynamic bearing considering five degree of freedom for a general rotor-bearing system. ASME J Tribol 121: 499–505

Jintanawan T (2000) Vibration of rotating disk/spindle systems with hydrodynamic bearings. PhD dissertation, University of Washington

Jintanawan T (2004) A model of distributed dynamic forces in herringbone grooved journal bearing. Proceedings of 1st International Conference on Advanced Tribology

Jintanawan T, Shen IY, Ku C-P (1999) Free and forced vibrations of a rotating disk pack and spindle motor system with hydrodynamic bearings. J Information Storage and Processing Systems 1:45–58

Jintanawan T, Shen IY, Tanaka K (2001) Vibration analysis of fluid dynamic bearing spindles with rotating-shaft design. IEEE Trans on Magn 37:799–804

Klit P, Lund JW (1986) Calculation of the dynamic coefficients of a journal bearing using a variational approach. ASME J Tribol 108: 421–425

Park JS, Shen IY, Ku C-P (2002) A parametric study on rocking vibration of rotating disk/spindle systems with hydrodynamic bearings. Microsyst Technol 8: 427–434

Shen IY; Ku C-P (1997) A nonclassical vibration analysis of multiple rotating disk/spindle system. ASME J Appl Mech 64: 165–174

Tseng CW; Shen JY; Shen IY (2003) Vibration of rotating-shaft HDD spindle motors with flexible stationary parts. IEEE Trans on Magn 39:794–799

Zirkelback N; San Andres L (1998) Finite Element analysis of herringbone grooved journal bearings: a parametric study. ASME J Tribol 120:234–240